# LATE-PLEISTOCENE WEDGE STRUCTURES ALONG THE PATAGONIAN COAST (ARGENTINA): CHRONOLOGICAL CONSTRAINTS AND PALAEO-ENVIRONMENTAL IMPLICATIONS

| | |
|---|---|
| Journal: | *Geografiska Annaler: Series A, Physical Geography* |
| Manuscript ID: | GAA1303-013.R3 |
| Wiley - Manuscript type: | Original Article |
| Date Submitted by the Author: | n/a |
| Complete List of Authors: | Ribolini, Adriano; University of Pisa, Department of Earth Sciences<br>Bini, Monica; University of Pisa, Department of Earth Sciences<br>Consoloni, Ilaria; University of Pisa, Department of Earth Sciences<br>Isola, Ilaria; National Institute of Geophysics and Volcanology,<br>Pappalardo, Marta; University of Pisa, Department of Earth Sciences<br>Zanchetta, Giovanni; University of Pisa, Department of Earth Sciences<br>Fucks, Enrique; Universidad Nacional de La Plata, Facultad de Ciencias Naturales y Museo<br>Panzeri, Laura; University of Milano Bicocca, Department of Material Sciences<br>Martini, Marco; University of Milano Bicocca, Department of Material Sciences<br>Terrasi, Filippo; University of Naples 2, Department of Environmental Sciences |
| Keywords: | ground wedge, Late-Pleistocene, Patagonian coast |
| Abstract: | This paper investigates several wedge structures formed in continental deposits covering marine sediments deposited during MIS 5 along the central Patagonian coast of Argentina. The size and surface microtexture characteristics of the infilling sediments are consistent with a depositional environment dominated by aeolian transport. Fragments of Andean volcanic rocks (glass shards) in the wedge-fill suggest long-distance transport via a westerly component of wind direction. The wedges are interpreted as products of deep seasonal frost action in frozen ground, which produced open cracks that filled rapidly with partially non-local aeolian sediments. Many wedges cross cut carbonate crusts that formed under permafrost conditions in coastal Patagonia. The radiocarbon dating of carbonate crusts yielded an age of 25-27 kyr BP, while wedge-fill sediments are OSL dated to 14,670 ± 750 yr BP. This indicates that ground wedge formation occurred during a cold event (the Antarctic Cold Reversal period) that interrupted the permafrost degradation following the Last Glacial Maximum. |
| | |

# LATE-PLEISTOCENE WEDGE STRUCTURES ALONG THE PATAGONIAN COAST (ARGENTINA): CHRONOLOGICAL CONSTRAINTS AND PALAEO-ENVIRONMENTAL IMPLICATIONS

ADRIANO RIBOLINI[1], MONICA BINI[1], ILARIA CONSOLONI[1], ILARIA ISOLA[2], MARTA PAPPALARDO[1], GIOVANNI ZANCHETTA[1], ENRIQUE FUCKS[3], LAURA PANZERI[4], MARCO MARTINI[4], FILIPPO TERRASI[5]

[1] Dipartimento di Scienze della Terra, University of Pisa, Pisa, Italy
[2] Istituto di Geofisica e Vulcanologia, Pisa
[3]Facultad de Ciencias Naturales y Museo, Universidad Nacional de La Plata, La Plata, Argentina
[4] Dipartimento di Scienza dei Materiali, University of Milano Bicocca, Milano, Italy
[5] Dipartimento di Scienze Ambientali, University of Naples 2, Napoli, Italy



ABSTRACT. This paper investigates several wedge structures formed in continental deposits covering marine sediments deposited during MIS 5 along the central Patagonian coast of Argentina. The size and surface microtexture characteristics of the infilling sediments are consistent with a depositional environment dominated by aeolian transport. Fragments of Andean volcanic rocks (glass shards) in the wedge-fill suggest long-distance transport via a westerly component of wind direction. The wedges are interpreted as products of deep seasonal frost action in frozen ground, which produced open cracks that filled rapidly with partially non-local aeolian sediments. Many wedges cross cut carbonate crusts that formed under permafrost conditions in coastal Patagonia. The radiocarbon dating of carbonate crusts yielded an age of 25-27 kyr BP, while wedge-fill sediments are OSL dated to 14,670 ± 750 yr BP. This indicates that ground wedge formation occurred during a cold event (the Antarctic Cold Reversal period) that interrupted the permafrost degradation following the Last Glacial Maximum.

## INTRODUCTION

This paper describes wedge structures in central Patagonia (latitude 46-48°S) (Fig. 1) and provides chronological constraints on wedge formation (OSL and $^{14}C$ dating). Late Pleistocene wedge structures have been documented in Tierra del Fuego (Coronato et al., 2004; Perez Alberti et al., 2008), the southern limit of Patagonia (Brockheim et al., 2009 and references therein), and northern Patagonia (Trombotto, 2002 and references therein). However, wedge features in Central Patagonia have received limited attention (e.g., Shellmann, 1998), and this is the first study to report wedge structures in the area of Puerto Deseado and the coast of San Jorge Gulf.

Many proxy records indicate that the Patagonian climate experienced cold events during deglaciation from the Last Glacial Maximum (LGM) (25-27 ka BP) (Kilian and Lamy, 2012 and references therein). These cold events are known to have affected Andean and piedmont areas of Patagonia, where palaeoclimatic information is abundant (Kilian and Lamy, 2012), and are known to have promoted glacial advances at comparable latitudes in the western Andes (Hein et al. 2010, García et al., 2012). However, terrestrial climate proxy records are limited in the Atlantic coastal lowlands of central Patagonia, and it is relatively unknown whether areas near the modern coast of central Patagonia were sensitive to the influence of the cold periods in the Late Pleistocene.

## PRESENT DAY CLIMATE

The climate of Puerto Deseado and San Jorge Gulf is semi-arid, cold-temperate and characterized by frequent strong winds (Coronato et al., 2008; Isla and Bujalesky, 2008). The climatic stations at of Comodoro Rivadavia and Puerto Deseado register less than 200 mm of rainfall per year, and have yearly average air temperatures of 13.0°C and 8.2°C, respectively. Summers (January-March) are relatively hot and dry, while winter months (June-August) are characterized by fresh/cold air temperatures (7°C and 4°C, respectively) (Servicio Meteorologico Nacional-Argentina, *http://www.smn.gov.ar*). Severe and frequent windstorms occur mainly during spring and summer (October and February, respectively), with wind speeds regularly exceeding 120 km $h^{-1}$. These windstorms can cause intense aeolian sediment transport, especially on unprotected soils. A strong, westerly component to wind direction is present throughout the area (del Valle et al., 2008; Sterk et al., 2012).

## GEOLOGICAL SETTING

Geologically, the San Jorge Gulf is situated between the Deseado Massif to the south and the Northern Massif to the north, both of which comprise Jurassic volcanic and volcano-clastic rocks (e.g., rhyolites, ignimbrites, and porphyroids). These massifs border the eastern termination of a predominantly extensional tectonic basin that trends East-West from the Andean belt to the Atlantic Ocean (Silwan, 2001).

The Pleistocene and Holocene sediments that outcrop along the Patagonian coast of San Jorge Gulf are predominantly of marine origin. The stratigraphy, palaeontology and geomorphology of these sediments have been studied widely (Bini et al., 2013; Shellmann and Radtke, 2010; Isola et al., 2011; Ribolini et al., 2011; Zanchetta et al., 2012; Zanchetta et al., in press and references therein). Particularly relevant here are gravel and sandy gravel marine deposits belonging to the MIS 5 transgression (ca. 125,000 yr BP) that are unconformably overlain by Holocene marine sandy gravel deposits. The latter contains abundant fossil remains indicative of a stormy beach environment. The Pleistocene units are mantled locally by a modern aeolian cover that reaches 2 m in thickness.

## WEDGE STRUCTURES



Sedimentary features indicative of frost wedge activity are observed along the San Jorge coast and in the area of Puerto Deseado (Fig. 1, Table 1). Morphologically, the features are regularly cuneiform to slightly irregular with wavy margins (Fig. 2a, b, c). The downward terminations are sharp, V-shaped, or curved upward and do not present a "beardy" margin (Fig. 2d, e). Maximum depths are 80-130 cm (with depths of approximately 80 cm being most common), while maximum widths range between 20 and 40 cm. In some locations, the features appear as thin, irregular, sinuous veins. Polygonal networks are visible on the surface only locally due to modern soil development and active aeolian deposition. The shape of the polygons is pseudo-hexagonal, with maximum diameters approximately 1.5-2 m (Fig. 2g).

The examined wedges started to form in the base of the aeolian cover or colluvial deposits (Fig. 2). Downward development of the wedge structures resulted in cross-cutting of massive horizons formed by continental depositional processes, composed of sand and sandy silt deposits with angular clasts in variable proportions. These horizons frequently contain rhizoconcretions and pedogenetic features, such as gypsum nodules and horizontal carbonate crusts, indicative of an arid depositional setting. In some instances, wedge development caused the downward displacement of host material inclusions, including fragments of carbonate crust (see also Fig. 9). No examples of deformation of sedimentary bedding were observed, nor were sorting effects observed that might reflect clast migration. Two generations of wedges are observed at some of the locations (Fig. 2f).

The best wedge structure development is observed at the Puerto Deseado and Cantera Delgado areas (Fig. 1), where wedges formed in thin colluvial and aeolian sediments that discontinuously mantled extensive Pleistocene marine sediments. A schematic geological background of both areas is reported in Fig. 3.

*Puerto Deseado*

Wedge features (Fig. 1) and polygonal cracks occurring near the surface (Fig. 2f) are observed in a section (Fig. 4) near the western margin of the Puerto Deseado village. At the base, the section comprises a fossiliferous marine gravel with sandy beds and pockets of weakly stratified sand inclined slightly seaward. The elevation of this layer (16-17 m above high tide water, hTw) is similar to that of the inner margin of the marine terraces near Puerto Deseado (Zanchetta et al., 2012) and is consistent with other data from the San Jorge Gulf (Rutter et al., 1989), allowing this deposit to be correlated with the MIS 5e highstand (ca. 125 ka).

A sharp unconformity marks the boundary between the marine gravel described above and a continental lithostratigraphic unit (17-17.6 m hTw) composed of massive silts and fine sands at the base and then by silt and clay with centimetre-scale horizontal layers of pedogenetic carbonate crust higher (Bk horizon). Considering the proximity to the fluvial valley of Río Deseado (Fig. 1), it is feasible that these sediments were deposited on a fluvial plain.

The unit above is conformably overlain by a matrix-supported deposit of angular bedrock fragments sustained by an unsorted coarse sand (17.6-18.2 m hTw). Subaerial slope processes (slope debris) can be invoked for the formation of this deposit. A poorly sorted, coarse-skewed and leptokurtic grey to pale-yellow fine-sand layer in the middle of the section, from 18.2 to 18.6 m hTw (WP301A in Fig. 5), is consistent with a partly reworked aeolian deposit. This unit contains visible wedge features (Fig. 4, see also Fig. 2e).

Vertical wedge development is from 80 to 120 cm, and the wedges feature clear lateral margins and sharp, V-shaped or curved-upward terminations. The upper limits of the wedges are coincident with, or very close to, the upper limit of the sandy layer in which they were hosted. The wedge infill deposits feature a massive structure without vertical cracks (Fig. 2e) and are composed of fine grain-sized sand, moderately sorted, with a symmetrical skewness and a mesokurtic kurtosis (WP301G, WP301H, Fig. 5).

Above the wedge-containing layer is a deposit composed of angular fragments of bedrock sustained by an unsorted coarse sand (18.6-19.4 m hTw). This unit is similar to that described in the 17.6-18.2 m hTw interval, and it can be interpreted analogously as slope debris involved in short and moderate transport.

The sandy layer in the 19.4-19.6 m hTw interval is cut by a second generation of wedge features (Fig. 2f) that, with respect to the first generation (see also Fig. 2e), are more numerous and present a regular lateral spacing of 2 to 3 m (Fig. 6). Vertical wedge dimensions range between 80 and 130 cm, with maximum widths of approximately 30 cm. The wedge margins are sharp and gently undulated, and the terminations are prevalently V-shaped. The tops of the wedges are situated near the base of the sandy layer described at 19.4-19.6 m hTw. Locally, vertical to steeply dipping cracks affect the wedges, dividing the sandy infillings into tabular elements (Fig. 6). The grain size corresponds to fine sand, moderately well sorted, with a symmetrical skewness and a mesokurtic kurtosis (WP301F, WP301K, WO301J) (Fig. 5).

The succession terminates with a dark brown Ah soil horizon, covered by aeolian and colluvial sands associated with present-day soil degradation.

SEM analysis to identify surface microtextures and therefore specific depositional environment were focused on the morphological characteristics of quartz grains from wedge infillings and the sandy host sediments. Wedge-fill grains ($1^{st}$ and $2^{nd}$ generation) are subrounded (Fig. 7a) and exhibit low-relief surfaces with rounded corners (Fig. 7b), dish-shaped depressions (up-turned plates) (Fig. 7c), silica precipitation and conchoidal fractures (Fig. 7d). Locally, crescentic, straight and arc-shaped steps, small scratches and 'breakage-block' features are observed (Fig. 7e, f). Volcanic glass shards are also observed in the wedge-fill, and these exhibit a quenching morphology that varies from pomiceous (oval and stretched vesicles) to bubble-wall (Fig. 7f, g), both of which are indicative of explosive eruptions with high fragmentation and dispersion. Additionally, some glass shard textures indicate shattering processes (Fig. 7h) that may be related to magma having made contact with glacier ice above. The rapid cooling of magma inhibited the development of vesicles and caused fractures due to thermal contraction.

*Cantera Delgado*

In the area of Caleta Olivia, several wedge features are found in sections along the coast. Wedges and other stratigraphic horizons are well preserved in a section situated a few kilometres south of Caleta Olivia, inside the quarry called Cantera Delgado (Shellmann, 1998) (Fig. 3b, Fig. 8).

At the base, the fossil-rich succession of crossbedded sand, containing decimetres-thick layers of gravel with sandy pockets, represents a Pleistocene marine unit and rests on a shore platform carved in volcanic bedrock. Electron Spin Resonance (ESR) ages of 95 and 75 Ka BP have been obtained from fossils collected from the top of this unit (Shellmann, 1998). Accordingly, MIS 5e (ca. 125 Ka BP) is considered feasible for the transgression phase that built this marine unit to a height of approximately 15 m hTw (Fig. 8).

The continental deposit resting on the MIS 5e gravel is composed of silty sands with dispersed pebbles and features horizontal pedogenetic carbonate crusts of 8-10 cm in thickness (Fig. 9). The wedge features visible in this layer are characterised by vertical development of 80-100 cm and maximum widths of 10-20 cm. The margins are undulated and the terminations are sharp and V-shaped. Although grain size was not determined analytically, visually, the infilling is sandy and finer than the hosting material. Wedge growth has cross cut the pedogenetic crust, causing a downward translation of some fragments of carbonate (Fig. 9).

The series continues upward with grey massive sands containing rhizoconcretions and pedogenetic carbonate nodules. This unit corresponds to aeolian sand cover. An Ah soil horizon terminates the succession, covered by loose deposits due to the present soil degradation caused by grazing and quarry activity.

## CHRONOLOGY

In the Puerto Deseado section, radiocarbon dating of the pedogenetic carbonate crust at 200 cm depth (Fig. 4) yielded an age of 25,780 ± 160 yr BP (30,404-30,774 cal yr BP) (WP301D). Dating of a crust cross cut by a sand wedge in the Cantera Delgado section yielded a similar age of 27,900 ± 320 yr BP (31,594-32,497 cal yr BP) (WP462B) (Figs. 8, 9 and Table 2). In both cases, the crust ages provide a maximum age of 25-27 ka BP for the timing of wedge development.

Radiocarbon ages obtained from pedogenetic carbonates do not necessarily represent the true age of formation if there has been incorporation of old limestone (e.g., Chen and Polach, 1986) or if $^{14}C$ activity in soil-respired $CO_2$ was lower compared to atmospheric $CO_2$ (Wang et al., 1994). In addition, redissolution and reprecipitation of calcite is possible after burial. The incorporation of old limestone or lower $^{14}CO_2$ activities would make the radiocarbon age appear older than the true age, whereas redissolution/reprecipitation processes may produce younger ages. Assuming no redissolution processes and that the incorporation of old limestone is improbable (due to the non-carbonate nature of the substrate host deposits), the ages of the pedogenic carbonates (Tab. 2) can be considered maximum ages of the samples.

In the Puerto Deseado section, samples for OSL dating were collected from the infill of a second-generation wedge and from the sandy host sediment at 115-160 cm depth (Fig. 4). The OSL age determination procedure is reported in the supplementary material. The results show that the first generation of wedges formed in a sandy layer that yielded an OSL age of 14,670 ± 750 yr BP (Table 3). Taking into account the uncertainties of the OSL age and accepting that frost cracking occurred subsequent to or syngenetically with host sediment deposition, an age of ca. 14-15 ka BP is proposed for the wedge formation.



## DISCUSSION

### *Wedge formation*

The wedge features studied along the San Jorge Gulf coast and in the Puerto Deseado area exhibited maximum vertical dimensions of approximately 1.5 m and were closely spaced (2-3 m). The polygonal networks on the surface were of similar dimensions (maximum diameters approximately 2 m). The infillings are consistently massive, without any vertical or steep laminations. Analyses of infilling sediments indicated fine sand (125-200 mm, 2-3 $\phi$), moderately sorted, with a symmetrical skewness and a mesokurtic kurtosis. These characteristics are consistent with a depositional environment dominated by aeolian transport and are consistent with grain-size curves for similar sediments in Patagonia (Smith et al., 2003; Zarate, 2003). The difference in grain-size between infillings and enclosing sediments is in many cases visually evident (e.g., Cantera Delgado), but is weak and limited in the degree of sorting and skewness for wedges formed in aeolian covers (e.g., Puerto Deseado).

Quartz grain microtextures, such as sub-rounded shapes, dish-shape concavities, rounded edges and polished surfaces, point to an aeolian depositional environment (Whalley and Langway, 1980; Sun et al., 2006). Some grain characteristics may also be interpreted as the effect of cryogenic weathering (i.e., conchoidal and breakage fractures)

(Wright et al., 1998; Sun et al., 1999; Frütsch, 2011; Woronko and Hoch, 2011). The existence of fragments of Andean volcanic rocks (glass shards) in the wedge infillings suggests long-distance transport (more than 650 km) in an eastward direction.

These data indicate that the wedge features reflect deep, seasonal frost action, with open cracks in the surface of a frozen ground that rapidly filled with sediments of not exclusively local derivation. The alternative process of desiccation cracking can be excluded because this type of cracking is uncommon in sand-sized materials (Allen, 1982), such as the sandy and gravelly sandy layers that host the observed wedges. Furthermore, wedge widths and depths observed are greater than those normally exhibited by desiccation cracking, which are generally less than 0.05 m and 0.25 m, respectively (Allen, 1982).

*Climatic and environmental implications*

A frost-wedge origin of the features means that the radiocarbon and OSL ages (Table 2, 3) indicate climatic conditions in the central Patagonian coast between 30 and 15 ka BP that were consistent with seasonally frozen ground. Previously, indurated carbonate crusts (*caliche*) along the Patagonian coast that are similar to those in Deseado and Delgado sections have been attributed to an arid and perennially frozen environment (permafrost) (del Valle and Beltramone, 1987; Vogt and del Valle, 1994).

Our study therefore indicates that a period of ground wedge formation most likely occurred at the end of a period of permafrost degradation following the LGM, when deep seasonal frost became the exclusive action affecting the subsurface under warmer conditions (e.g., French et al. 2009). It is possible that frost cracking of both the seasonally frozen layer and the perennially frozen sediment beneath may have occurred in some locations, but evidence for wedge formation under permafrost conditions is currently lacking.

Terrestrial and oceanic proxy records for the southern hemisphere indicate that the deglaciation following the LGM (23-25 Ka BP) experienced an Antarctic pattern, which is characterized by a temperature plateau or a reversal trend in the 12.5-15 ka BP interval (Antarctic Cold Reversal, ACR) (Fig. 10). Cold temperatures and pronounced aridity during the ACR period are demonstrated by glacial advances (Kaplan et al., 2011; Garcia et al., 2012), desiccation of lakes (i.e., Lago Cardiel) (Stine and Stine, 1990), and pollen records indicative of a treeless, and open (tundra-like) landscape dominated by eurythermal herbs and shrubs (Markgraf and Huber, 2010). In this respect, our results support the hypothesis that the present coastal environment of the Central Patagonia, similar to more internal regions, also reacted to the lower ACR temperatures and higher aridity, promoting deep seasonal frost cracks that filled with aeolian sediments. The coastal area would therefore have been characterized by conditions conducive to frost cracking (Svensson, 1988; Burn, 1990), including scarce vegetation, limited persistence of the seasonal snow cover, and a mean annual air temperature at least 10°C lower than today. These environmental conditions are consistent with a continental lowland hundreds of kilometres inland from the coast, as the studied area was during the Late Pleistocene. Furthermore, the presence of volcanic glass shards of Andean provenance in the wedge-fill of volcanic glass shards of Andean provenance demonstrates the influence on the Patagonian coast of the South Western Wind (SWW) atmospheric current, which, during the ACR, promoted long-distance transport of sediment. More specifically, the radiocarbon-dated Reclús eruption at 14,900 yr BP (Haberzettl et al., 2009) may be the source of the volcanic fragments in the studied sand wedges, although further work using micro-analytical techniques would be required to confirm this hypothesis.

## CONCLUSION

Ground wedge structures in the continental deposits that cover MIS 5 marine sediments in the region of Puerto Deseado and the San Jorge Gulf are indicative of frost cracking in seasonally frozen ground. Sedimentological evidence has verified this thermal condition at several locations along the Argentinean coast of Patagonia between latitudes 46 and 48°S and complements existing evidence of even colder ground thermal conditions (i.e., permafrost) from locations further south and in Tierra del Fuego (Coronato et al., 2004; Bockheim et al., 2009).

Furthermore, ages of carbonate crusts and ground wedge formation provide evidence of long-term climatic warming that saw deep seasonal frost becoming the dominant process at the end of a period of permafrost degradation beginning after the LGM.

Geological and geomorphological evidence from the Patagonian coast region has traditionally been exploited to provide palaeoenvironmental archives of sea level oscillations and the oceanic conditions (i.e., temperature and salinity) registered by marine fauna (e.g., Schellmann and Radtke, 2010). In contrast, published evidence for climate-driven continental processes is less common, especially in the context of the Late

Pleistocene. The evidence presented in this paper that documents the ACR-related decrease/reversal in temperature following the LGM is therefore unusual. Furthermore, it indicates the potential to improve land-based records of Late Pleistocene climate and environmental changes in this region using geomorphological approaches. In particular, the grain-size composition of wedge infill indicates relatively dry aeolian processes and a westerly component in the dominant winds that allowed the products of Late Glacial eruptions to reach the present Patagonian coast.

**Acknowledgements**

Discussions with Prof. Emeritus Hughes French greatly improved the manuscript and we thank Prof. A. Coronato and Prof. E. Kolstrup for their insightful reviews. We would like also to acknowledge Prof. D. Swift for useful suggestions and final review. The professional editing services of the American Journal Experts provided an English revision of the manuscript. This work was made possible thanks to the funding of the University of Pisa (Progetto Ateneo 2007, Leader G. Zanchetta) and MIUR (PRIN2008, Leader G. Zanchetta). We thank J. Cause and the CADACE no-profit organization for providing logistical support to the field campaign.

*Adriano Ribolini, Monica Bini, Ilaria Consoloni, Ilaria Isola, Marta Pappalardo, Giovanni Zanchetta, Dipartimento di Scienze della Terra, University of Pisa, Pisa, Italy*
*E-mail: ribolini@dst.unipi.it*

*Enrique Fucks Facultad de Ciencias Naturales y Museo, Universidad Nacional de La Plata, Paseo del Bosque s/n, B1900FWA, La Plata, Argentina*

*Marco Martini, Laura Panzeri, Dipartimento di Scienza dei Materiali, University of Milano Bicocca, Via Roberto Cozzi 53 - 20125, Milano, Italy*

*Filippo Terrasi Dipartimento di Scienze Ambientali, University of Naples 2, Via Vivaldi 43 - 81100 Caserta, Italy*

REFERENCES

Allen, J.R.L., 1982. Sedimentary Structures: their Character and Physical Basis. Developments in Sedimentology, 30B. Elsevier, Amsterdam, 663 pp.

Bini, M., Consoloni, I., Isola, I., Pappalardo, M., Ragaini, L., Ribolini, A. and Zanchetta, G. Markers of palaeo sea-level in rocky coasts of Patagonia (Argentina). *Rendiconti Online della Società Geologica Italiana*, 20, 10-14.

Blott, S.J. and Pye K., 2001. GRADISTAT: a grain size distribution and statistics package for the analysis of unconsolidated sediments. *Earth Surface Processes and Landforms*, 26, 11,1237–1248.

Bockheim, J., Coronato, A., Rabassa, J., Ercolano, B. and Ponce, J. 2009. Relict sand wedges in southern Patagonia and their stratigraphic and paleo-environmental significance. *Quaternary Science Reviews*, 28,1188–1199.

Chen, Y., Polach, H., 1986. Validity of 14C ages of carbonate sediments. *Radiocarbon*, 28, 464-472.

Coronato, A., Bujalesky, G., Pérez Alberti, A. and Rabassa, J., 2004. Evidencias criogénicas fósiles en depósitos marinos interglaciarios de Tierra del Fuego, Argentina. *X Reunión Argentina de Sedimentología*, *Acta de Resúmenes,* San Luis, Argentina, 48-49.

Coronato, M.J.; Coronato, F., Mazzoni, E. and Vásquez, M., 2008. The Physical Geography of Patagonia and Tierra del Fuego In: Rabassa, J. (ed.), *Late Cenozoic of Patagonia and Tierra del Fuego*. Elsevier, Amsterdam.13-55.

del Valle, H.F., Rostagno, C.,M., Coronato, F.,R., Bouza, P.J. and Blanco, P.,D. 2008. Sand dune activity in north-eastern Patagonia. *Journal of Arid Environments* 72, 411–422.

del Valle, H. and Beltramone, C., 1987. Morfología de las acumulaciones calcáreas en algunos paleosuelos de Patagonia Oriental (Chubut). *Ciencia del Suelo,* 5, 77–87.

Fogwill, C.,J. and Kubick, P.,W. 2005. Glacial stage spanning the Antarctic cold reversal in Torres del Paine (511S), Chile, based on preliminary cosmogenic exposure ages. *Geografiska Annaler*, 87A, 403–408.

French, H., Demitroff M. and Newell, W.L., 2009. Past Permafrost on the Mid-Atlantic Coastal Plain, Eastern United States. *Permafrost and Periglacial Processes*, 20, 285–294

Frütsch, F., 2011. *Quartz grain weathering in a periglacial environment: indications from SEM and TEM studies using single grain features*. Master thesis, Fachbereich Geowissenschaften, Freie Universität Berlin, Germany, hdl:10013/epic.39487, 20 January 2013.

García, J.L., Kaplan, M.R., Hall, B.L., Schaefer, J.M., Vega, R.,M., Schwartz, R. and Finkel, R. 2012. Glacier expansion in southern Patagonia throughout the Antarctic cold reversal. *Geology*, doi: 10.1130/G33164.1.

Glasser, F.G., Harrison, S., Schnabel, C., Fabel, D. and Jansson, K.N., 2012. Younger Dryas and early Holocene age glacier advances in Patagonia. *Quaternary Science Reviews*, 58, 7-17.

Haberzettl, T., Anselmetti, F.,S., Bowen, S.W., Fey, M., Mayr, C., Zolitschka, B., Ariztegui, D., Mauz, B., Ohlendorf, C., Kastner, S., Lücke, A., Schäbitz, F., and Wille, M., 2009. Late Pleistocene dust deposition in the Patagonian steppe e extending and refining the paleoenvironmental and tephrochronological record from Laguna Potrok Aike back to 55 ka. *Quaternary Science Reviews,* 28 (25-26), 2927-2939.

Hein, A.,S., Hulton, N.,R.,J., Dunai, T.,J., Sugden, D.,E, Kaplan, M.,R. and Xu, S. 2010. The chronology of the Last Glacial Maximum and deglacial events in central Argentine Patagonia. *Quaternary Science Reviews*, 29, 1212–1227.

Isla, F.I. and Bujalesky, G.G., 2008. Coastal Geology and Morphology of Patagonia and the Fuegian Arcipelago. In: Rabassa ,J., (ed.), *Late Cenozoic of Patagonia and Tierra del Fuego*, Elsevier, Amsterdam. 227-239.

Isola, I., Bini, M., Ribolini, A., Pappalardo, M., Consoloni, I., Fucks, E., Boretto, G., Ragaini, L. and Zanchetta, G., 2011. Geomorphologic Map of Northeastern Sector of San Jorge Gulf (Chubut, Argentina). *Journal of Maps*, 476-486.

Jouzel, J., Masson-Delmotte, V., Cattani, O., Dreyfus, G., Falourd, S., Hoffmann, G., Minster, B., Nouet, J., Barnola, J.,M., Chappellaz, J., Fischer, H., Gallet, J.C., Johnsen, S., Leuenberger, M., Loulergue, L., Luethi, D., Oerter, H., Parrenin, F., Raisbeck, G., Raynaud, D., Schilt, A., Schwander, J., Selmo, E., Souchez, R., Spahni, R., Stauffer, B., Steffensen, J.,P., Stenni, B., Stocker, T.F., Tison, J.L., Werner, M. and Wolff, E.W., 2007. Orbital and millennial Antarctic climate variability over the past 800,000 years. *Science,* 317 (5839), 793-796.

Kaplan, M.R., Strelin, J.A., Schaefer, J.M., Denton, G.,H., Finkel, R.,C., Schwartz, R., Putnam, A.,E., Vandergoes, M.J., Goehring, B.M., and Travis S.G., 2011. In-situ cosmogenic 10Be production rate at Lago Argentino, Patagonia: implications for lateglacial climate chronology*. Earth and Planetary Science Letters*, 309 (1-2), 21-32.

Kilian, R. and Lamy, F., 2012. A review of Glacial and Holocene palaeoclimate records from southernmost Patagonia (49-55 °S). *Quaternary Sciences Reviews*, 53, 1-23.

Lemieux-Dudon, B., Blayo, E., Petit, J.-R.,Waelbroeck, C., Svensson,A., Ritz, C., Barnola, J.M., Narcisi, B. and Parrenin, F., 2010. Consistent dating for Antarctic and Greenland ice cores. *Quaternary Sciences Reviews* 29, 8–20.

Markgraf, V., Huber, U.M., 2010. Late and postglacial vegetation and fire history in Southern Patagonia and Tierra del Fuego. *Paleogeography, Paleoclimatology, Paleoecology*, 297, 351-366.

Moreno, P.M., Kaplan, M.R., François, J.P., Villa-Martinez, R., Moy, C.M., Stern, C.R. and Kubik, P.W. 2009. Renewed glacial activity during the Antarctic Cold Reversal and persistence of cold conditions until 11.5 ka in SW Patagonia. *Geology*, 37, 375–378.

Perez-Alberti, A., Valcarcel Díaz, M., Coronato, A., Rabassa, J., Costa Casais, M., 2008. Wedge structures in southernmost Argentina (Río Grande, Tierra del Fuego). *Ninth International Conference on Permafrost*, Fairbanks, Proceeding 1381-1385

Putnam, A., Schaefer, J., Barrell, D.J.A., Vandergoes, M., Denton, G.H., Kaplan, M., Finkel, R.C., Schwartz, R., Goehring, B.M., and Kelley, S., 2010. In situ cosmogenic 10Be production-rate calibration from the Southern Alps, New Zealand. *Quaternary Geochronology*, 5, 392–409.

Reimer, P.J., Baillie, M.G.L., Bard, E., Bayliss, A., Beck, J.W., Blackwell, P.G., Bronk Ramsey, C., Buck, C.E., Burr, G.S., Edwards, R.L., Friedrich, M., Grootes, P.M., Guilderson, T.P., Hajdas, I., Heaton, T.J, Hogg, A.G., Hughen, K.A., Kaiser, K.F., Kromer, B., McCormac, F.G., Manning, S.W., Reimer, R.W., Richards, D.A., Southon, J.R., Talamo, S., Turney, C.S.M., van der Plicht, J., Weyhenmeyer, C.E. 2009. IntCal09 and Marine09 radiocarbon age calibration curves, 0–50,000 years cal BP. *Radiocarbon* 51, 1111–1150.

Ribolini, A., Aguirre, M., Baneschi, I., Consoloni, I., Fuck, E., Isola, I., Mazzarini F., Pappalardo, M., Zanchetta, G. and Bini, M. 2011. Holocene beach ridges and coastal evolution in the Cabo Raso Bay (Atlantic Patagonian Coast, Argentina). *Journal of Coastal Research*, 27, 973-983.

Rutter, N., Schnack, E.J., Fasano, J.L., Isla, F.I., del Rio, J., Radtke, U., 1989. Correlation and dating of Quaternary littoral zones along the coast of Patagonia and Tierra del Fuego. *Quaternary Science Reviews* 8, 213-234.

Schellmann, G., 1998. Jungka¨nozonische Landschaftsgeschichte patagoniens (Argentinien). Andine Vorlandvergletchenrungen, Talentwicklung und marine Terrassen. *Essener Geographische Arbeiten*, 29, Essen, Germany.

Schellmann, G. and Radtke, U., 2010. Timing and magnitude of Holocene sea-level changes along the middle and south Patagonian Atlantic coast derived from beach ridge systems, littoral terraces and valley-mouth terraces. *Earth-Science Reviews,* 103, 1–30.

Smith, J., Vance, D., Kemp, R. A., Archer, C., Toms, P., King, M. and Zarate, M., 2003. Isotopic constraints on the source of Argentinean loess-with implication for atmospheric circulation and provenance of Antarctic dust during recent glacial maxima. *Earth and Planetary Science Letters*, 212, 181-196.

Stenni, B., Jouzel, J., Masson-Delmotte, V., Röthlisberger, R., Castellano E., Cattani, O., Falourd, S., Johnsen, S.J., Longinelli, A., Sachs, J.P., Selmo, E., Souchez, R., Steffensen, J.P. and Udisti, R., 2004. *Earth and Planetary Science Letters*, 217, 1–2, 183-195.

Sterk G., Parigiani J., Cittadini E., Peters P., Scholberg J. and Peri, P., 2012. Aeolian sediment mass fluxes on a sandy soil in Central Patagonia. *Catena*, 95, 112–123.

Stine S. and Stine, M., 1990. A record form Lake Cardiel of climate change in southern South America. *Nature*, 345, 705-708.

Sun, J.M., Ding, Z.L., Liu, T.S., Rokosh, D. and Rutter, N., 1999. 580,000-Year environmental reconstruction from aeolian deposits at the Mu Us Desert margin, China. *Quaternary Science Reviews*, 18, 1351–1364.

Sun, J.M., Li, S.H., Han, P. and Chen, Y.Y., 2006. Holocene environmental changes in the central Inner Mongolia, based on single-aliquot-quartz optical dating and multi-proxy study of dune sands. *Palaeogeography, Palaeoclimatology, Palaeoecology,* 233, 51–62.

Terrasi, F., De Cesare, N., D'Onofrio, A, Lubritto, C., Marzaioli, F., Passariello, I., Rogalla, D., Sabbarese, C., Borriello, G., Casa, C. and Palmieri, A., 2008. High precision 14C AMS at CIRCE. *Nuclear Instruments and Methods in Physics Research*, B 266(10), 2221–4.

Trombotto, D., 2002. Inventory of fossil cryogenic forms and structures in Patagonia and the mountains of Argentina beyond the Andes. *South American Journal of Earth Sciences*, 98, 171- 180.

Vogt, T. and del Valle, H.F. 1994. Calcretes and cryogenic structures in the area of Puerto Madryn (Chubut, Patagonia, Argentina). *Geografiska Annaler*. 76A, 57–75.

Whalley, W.B. and Langway, C.C., 1980. A Scanning Electron Microscope Examination of Subglacial Quartz Grains from Camp Century Core, Greenland – A Preliminary Study. *Journal of Glaciology*, 25, 91, 125–132.

Woronko, B. and Hoch, M., 2011. The development of frost-weathering micorstruttures on sand-sized quartz grains: examples from Poland and Mongolia. *Permafrost and Periglacial Processes*, 22, 214-227.

Wang Y., Amudson R., Trumbore S. 1994. A model of $^{14}CO^{2}$ and its implications for using 14C to date pedogenic carbonate. *Geochimica et Cosmochimica Acta*, 58, 393-399.

Wright, J., Smith, B. and Whalley, B., 1998. Mechanism of loess-sized quartz silt production and their relative effectiveness: laboratory simulations. *Geomorphology,* 23,15-34

Zanchetta, G., Consoloni, I., Isola, I., Pappalardo, M., Ribolini A., Aguirre, M., Fucks E., Baneschi, I., Bini, M., Mazzarini, F., Ragaini, L. and Terrasi, F., 2012. New insight on the Holocene marine transgression in the Bahia Camarones (Chubut, Argentina). *Italian Journal of Geosciences*, 131, 19-31.

Zanchetta, G., Bini, M., Isola, I., Pappalardo, M., Ribolini, A., Consoloni, I., Boretto, G., Fucks, E., Ragaini, L. and Terrasi, F., in press. Middle to Late Holocene relative sea level changes at Puerto deseado (Patagonia, Argentina). *The Holocene*, in press.

Zarate, M.A., 2003. Loess of southern South America. Quaternary Sciences reviews 22, 1987-2006.

CAPTIONS

Figure 1. Sketch map of the central Patagonian coast. Ground wedges were observed at sites indicated by a black circle/code. The codes are used in the captions of subsequent Figures to indicate location.

Figure 2. Example ground wedge morphology along San Jorge Gulf and Puerto Deseado area. (a) V-shaped with undulated margins. The wedge is formed in a sandy deposit and cross-cut a colluvial layer beneath (WP462). (b), (c) V-shaped with undulated and regular margins. (b) is formed in a sandy deposit and cross cuts a colluvial layer beneath (WP510); (c) is formed in a sandy deposit and cross cuts a sandy layer with interspersed angular clasts (WP546). (d) V-shaped with undulated margins and vertical dipping crack. The wedge is formed in a gravelly-sandy layer (WP348). (e) Regular margin and concave upward termination. The wedge is formed in a sandy layer and cross-cut unsorted sands with interspersed angular clasts (WP301). (f) Two generations of wedges formed in a sandy layer and cross-cutting unsorted sands with interspersed angular clasts. The lower wedge is the same shown in (e) (WP301). (g) Polygonal network (note the knife for scale) (WP327).

Figure 3. Simplified geological maps of the Puerto Deseado (a) and Cantera Delgado (b) areas. 1: bedrock (volcanic rocks); 2: Pleistocene marine deposits (MIS 5e); 3: Holocene marine deposits; 4: Holocene aeolian cover; 5: urbanized area; 6: quarry.

Figure 4. The Puerto Deseado schematic section (WP301) where several wedges were observed. 1: Clinostratified gravel with marine fossils; 2: massive and cohesive silt; 3: sand; 4: silt and clay with horizons of pedogenetic carbonate crusts (in gray); 5: unsorted sand with interspersed angular clasts; 6: Soil, Ah horizon; 7: wedge. Elevations are above the high tide water (hTw).

Figure 5. Grain size analyses. (a) Clay-silt-sand triangular diagram, showing the grain-size composition of the samples. An enlargement of the sand field is shown (upper left corner). (b) Grain size distribution of Sample 301A obtained from host sediment at WP301; the other distributions are for samples from the wedge infillings. Statistics obtained using GRADISTAT (Blott and Pye, 2001).

Figure 6. Ground wedges of second generation in the Puerto Deseado section (WP327).

Figure 7. SEM imagines illustrating the morphology of quartz grains of the ground wedge infillings. (a) Subrounded grains. (b) Subrounded grain with scratches and low relief surface locally plastered by silica precipitation. (c) Subrounded grain, with dish-shaped concavities and silica precipitations. (d) Conchoidal fractures and breakage block features. (e) Subrounded grain with crescent steps. Pumiceous glass-shard with stretched vesicles. (f) Irregular grain with a breakage block feature. (g) Shattered glass-shard. (h) Bubble-wall glass-shard.

Figure 8. The Cantera Delgado section (WP461) (not to scale). 1: bedrock; 2: Pleistocene marine deposits; 3: Holocene marine deposits; 4: Holocene continental deposits; 5: soil; 6: quarry waste deposit. See the text for a detailed litostratigraphic description. The radiocarbon age of the pedogenetic carbonate crust is indicated. An enlargement of the sand wedge is shown in Fig. 9. Elevations are above the high tide water (hTw).

Figure 9. Detail of sand wedge from Fig. 8. Host material (pedogenetic crust) has moved downward as the wedge has developed. The crust yielded an OSL age of 27,900 ± 320 yrs BP.

Figure 10. Sand wedge age (red triangle, SW) (this work) in the context of palaeoclimate information for Patagonia. Alkenone Sea Surface Temperature records are from the South Pacific cores ODP 1233 and MD07-3128. Antarctic surface temperature changes (EDC) (deviation from

mean of the last millenium; Jouzel et al., 2007) plotted on the Lemieux-Dundon time-scale (Lemieux-Dundon et al., 2010). Changes of the isotopic fractionation of hydrogen in water (ice) measured at the ice core EPICA Dome C (Antarctic) (Stenni et al., 2004). Surface exposure ages of glaciers advances (blue points with uncertainty bar). LP: Lago Pueyrredon (Hein et al. 2010); LBA: Lago Buenos Aires (Hein et al. 2010); TP: Torres del Paine (Moreno et al., 2009; Fogwill and Kubick, 2005; García et al., 2012); NPI: North Patagonian Icefield (West to the Lago Buenos Aires) (Glasser at al., 2012). Ages were calculated with the Dunai time-dependent scaling scheme, adopting the isotopic production rate tested for South America (Putnam et al., 2010). YD = Younger Dryas, ACR = Antarctic Cold Reversal. In the map: SJG = St Jorge Gulf, PD = Puerto Deseado, LC = Lago Cardiel.

| Site code | Latitude (S) | Longitude (W) | Elevation (m asl) |
|---|---|---|---|
| WP301 | 47°45'03" | 65°54'54" | 19 |
| WP311 | 47°43'11" | 65°50'28" | 9 |
| WP327 | 47°45'18" | 65°53'33" | 9 |
| WP348 | 47°42'22" | 65°49'57" | 11 |
| WP404 | 47°30'50" | 66°06'12" | 115 |
| WP405 | 47°23'48" | 66°03'52" | 117 |
| WP425 | 47°44'38" | 65°55'45" | 31 |
| WP43A | 47°45'15" | 65°54'23" | 12 |
| WP73A | 47°45'04" | 65°53'39" | 21 |
| WP462 | 46°33'31" | 67°25'57" | 18 |
| WP471 | 46°23'18" | 67°32'51" | 29 |
| WP508 | 46°08'36" | 67°37'50" | 32 |
| WP510 | 46°07'47" | 67°37'49" | 26 |
| WP546 | 46°28'05" | 67°30'59" | 51 |
| WP582 | 45°29'53" | 67°35'52" | 652 |

Table 1. Sites at which ground wedges were observed.

| Sample | Site code | $^{14}C$ yr BP measured ages | $^{14}C$ cal yr BP (±1σ) | Species or Material |
|---|---|---|---|---|
| DSH1964 | WP 301D | 25,780±160 | 30,404 - 30,774 | Pedogenic carbonate |
| DSH4033 | WP 462B | 27,900±320 | 31,594 - 32,497 | Pedogenic carbonate |

Table 2. Radiocarbon ages obtained for this study. Ages were measured at the CIRCE laboratory of Caserta (Italy) (Terrasi et al., 2008). Calibration has been performed using INTCAL09.14c data set in CALIB 6 (Reimer et al, 2009).

| Sample | Water content (%) | $D_e$ (Gy) | ppm U | ppm Th | ppm $^{40}$K | Dose rate (mGy/a) | Age (a) |
|---|---|---|---|---|---|---|---|
| WP301B | 23 ± 1 | 33 ± 2 | 1.91 ± 0.09 | 6.02 ± 0.30 | 1.91 ± 0.06 | 2.25 ± 0.07 | 14,670 ± 750 |
| WP301C | 24 ± 1 | | 1.44 ± 0.07 | 4.54 ± 0.20 | 1.91 ± 0.06 | 2.14 ± 0.06 | not datable |

Table 3. Summary data for OSL ages obtained for this study. See supplementary information for details on the OSL procedure.

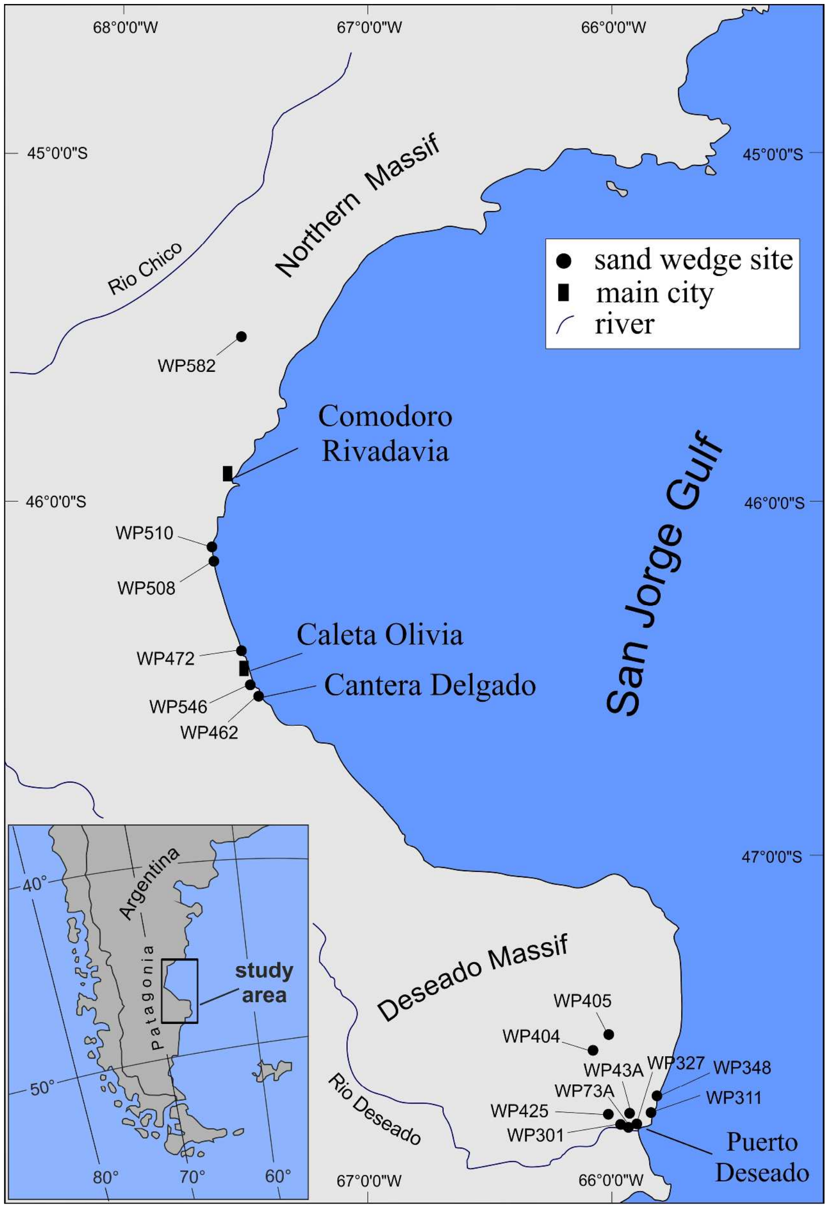


Sketch map of the central Patagonian coast. Ground wedges were observed at sites indicated by a black circle/code. The codes are used in the captions of subsequent Figures to indicate location.
127x185mm (600 x 600 DPI)

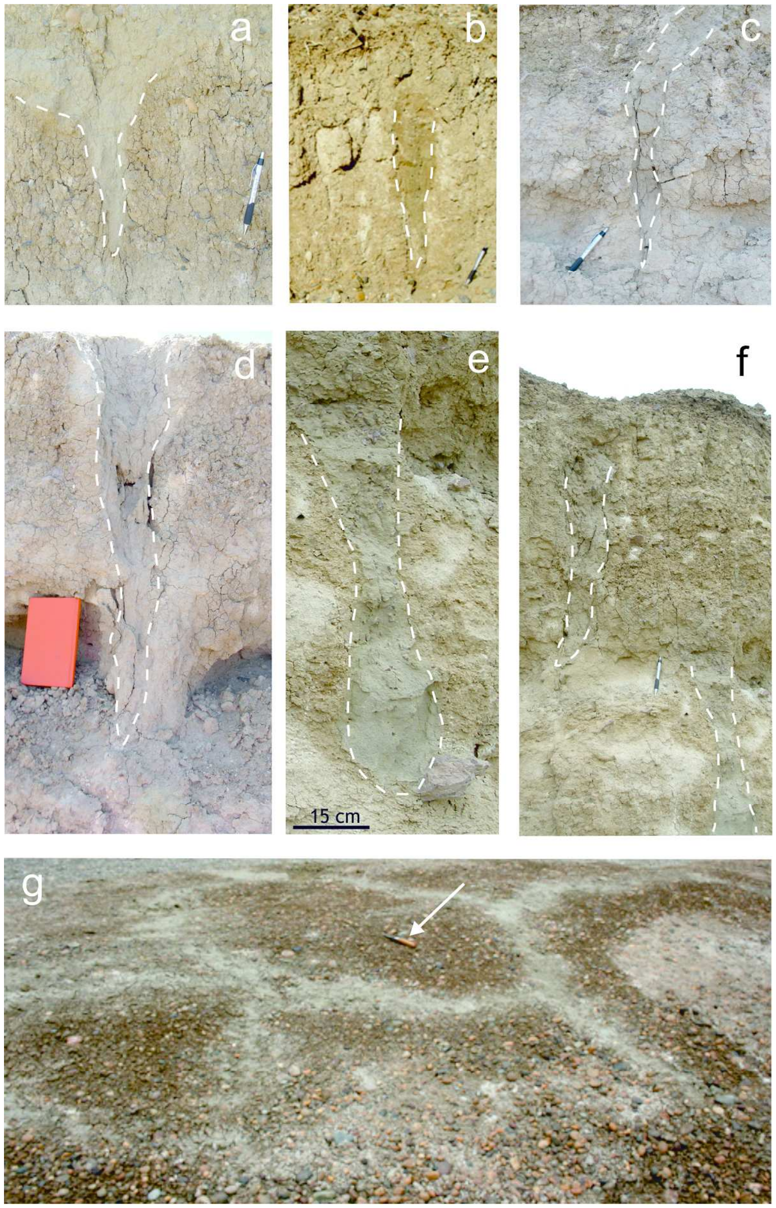


Example ground wedge morphology along San Jorge Gulf and Puerto Deseado area. (a) V-shaped with undulated margins. The wedge is formed in a sandy deposit and cross-cut a colluvial layer beneath (WP462). (b), (c) V-shaped with undulated and regular margins. (b) is formed in a sandy deposit and cross cuts a colluvial layer beneath (WP510); (c) is formed in a sandy deposit and cross cuts a sandy layer with interspersed angular clasts (WP546). (d) V-shaped with undulated margins and vertical dipping crack. The wedge is formed in a gravelly-sandy layer (WP348). (e) Regular margin and concave upward termination. The wedge is formed in a sandy layer and cross-cut unsorted sands with interspersed angular clasts (WP301). (f) Two generations of wedges formed in a sandy layer and cross-cutting unsorted sands with interspersed angular clasts. The lower wedge is the same shown in (e) (WP301). (g) Polygonal network (note the knife for scale) (WP327).
205x321mm (300 x 300 DPI)

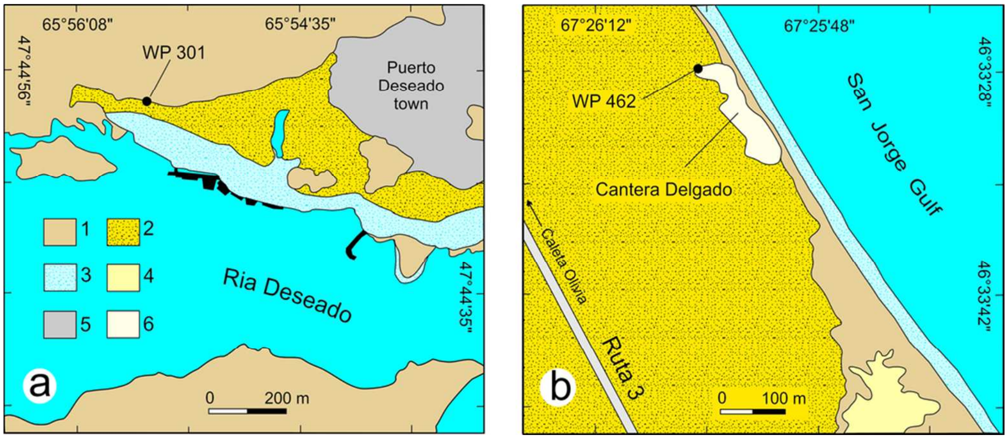


Simplified geological maps of the Puerto Deseado (a) and Cantera Delgado (b) areas. 1: bedrock (volcanic rocks); 2: Pleistocene marine deposits (MIS 5e); 3: Holocene marine deposits; 4: Holocene aeolian cover; 5: urbanized area; 6: quarry.
92x39mm (300 x 300 DPI)

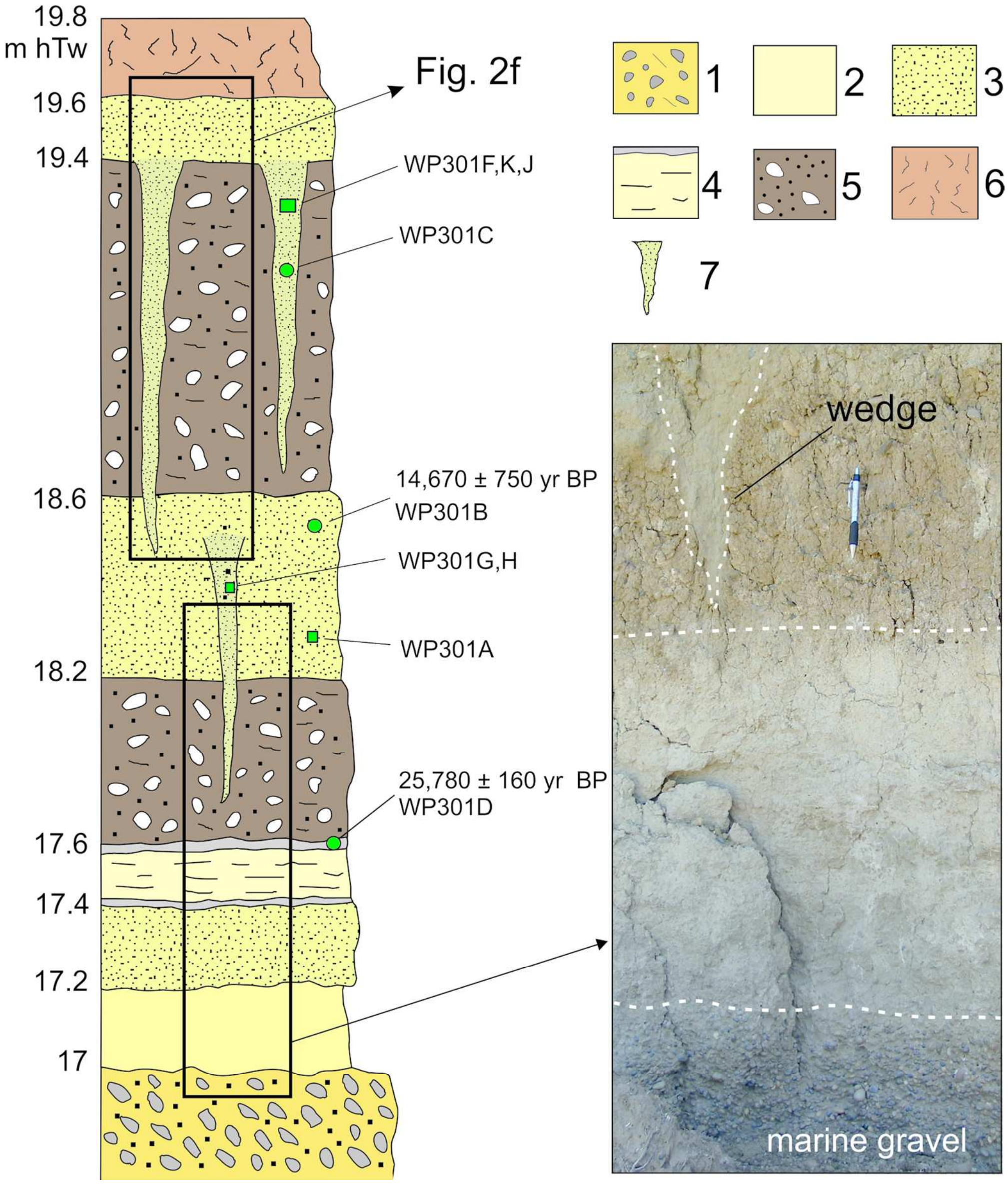


The Puerto Deseado schematic section (WP301) where several wedges were observed. 1: Clinostratified gravel with marine fossils; 2: massive and cohesive silt; 3: sand; 4: silt and clay with horizons of pedogenetic carbonate crusts (in gray); 5: unsorted sand with interspersed angular clasts; 6: Soil, Ah horizon; 7: wedge. Elevations are above the high tide water (hTw).
149x175mm (300 x 300 DPI)

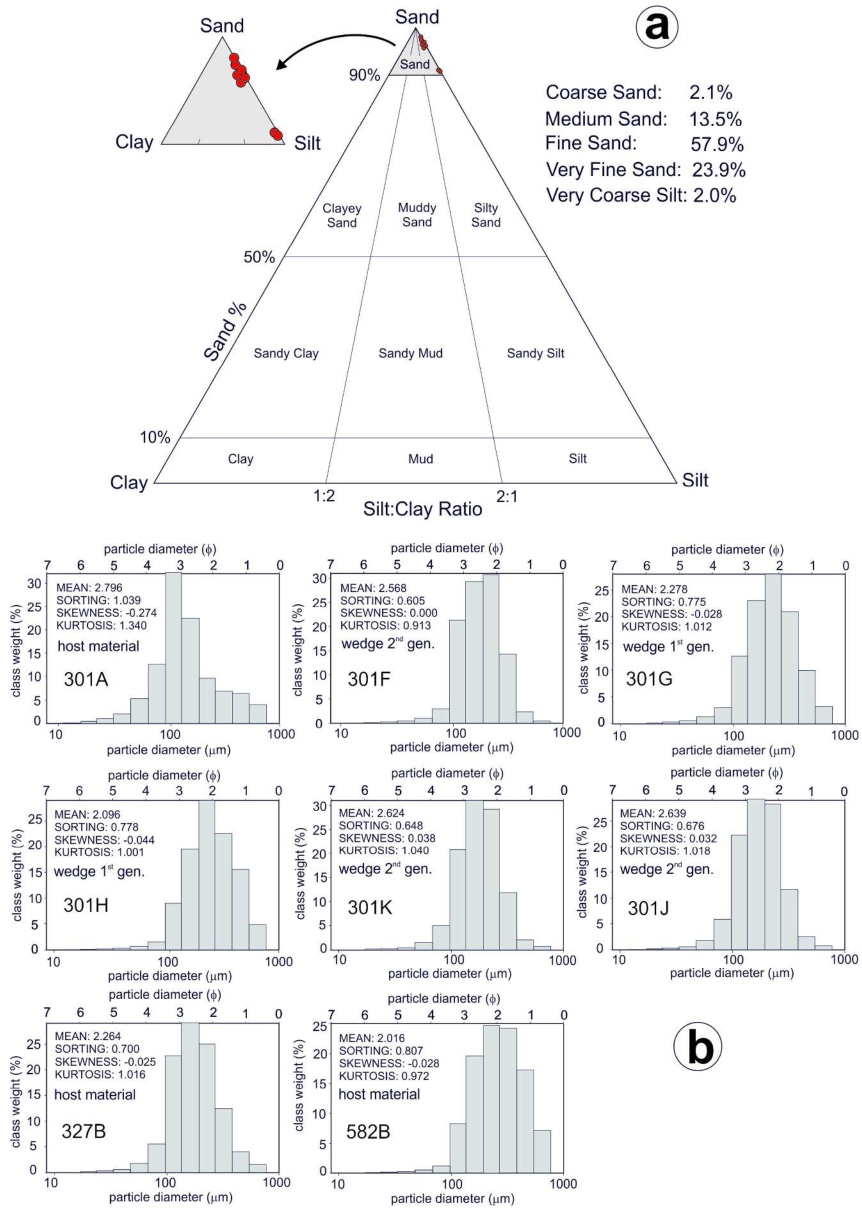


Grain size analyses. (a) Clay-silt-sand triangular diagram, showing the grain-size composition of the samples. An enlargement of the sand field is shown (upper left corner). (b) Grain size distribution of Sample 301A obtained from host sediment at WP301; the other distributions are for samples from the wedge infillings. Statistics obtained using GRADISTAT (Blott and Pye, 2001).
189x267mm (300 x 300 DPI)

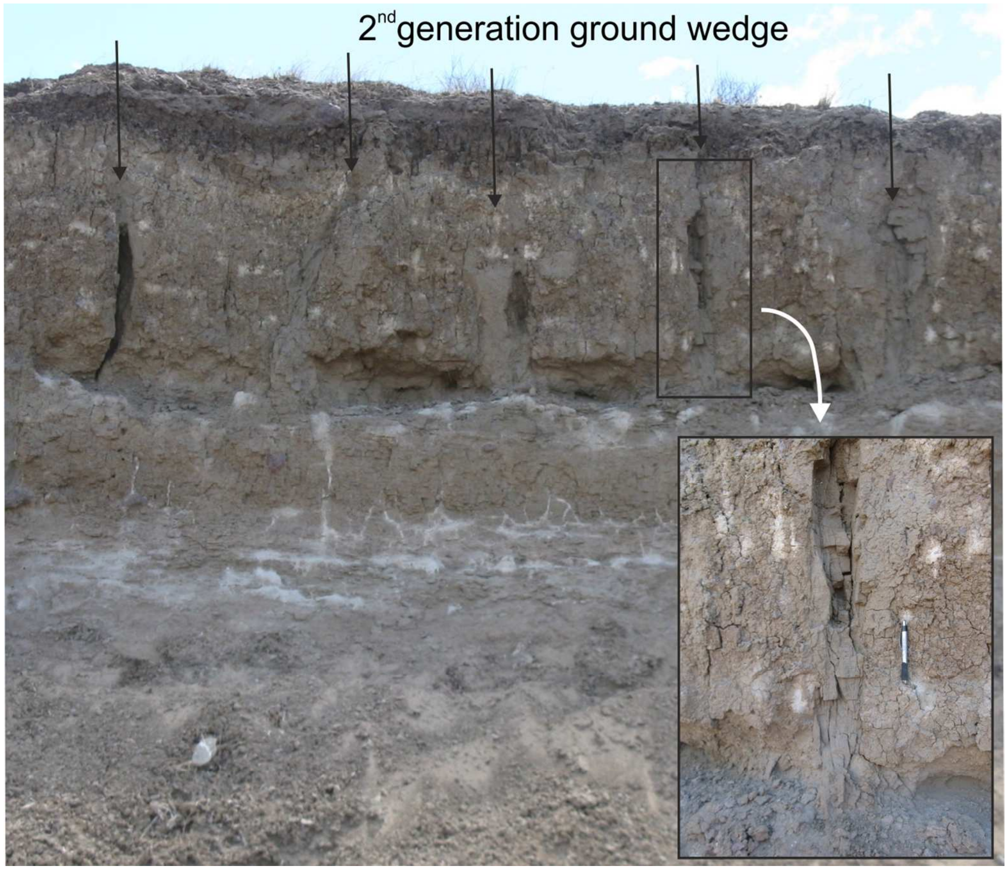


Ground wedges of second generation in the Puerto Deseado section (WP327).
122x105mm (300 x 300 DPI)

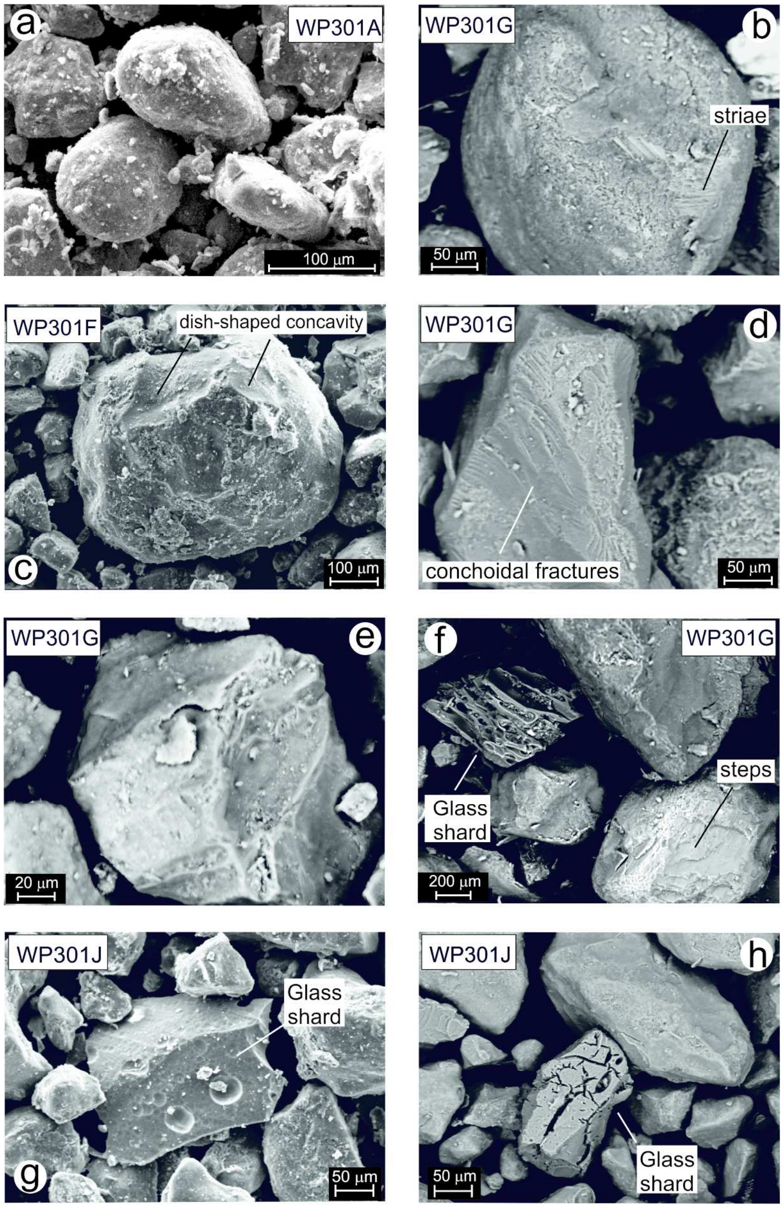


SEM imagines illustrating the morphology of quartz grains of the ground wedge infillings. (a) Subrounded grains. (b) Subrounded grain with scratches and low relief surface locally plastered by silica precipitation. (c) Subrounded grain, with dish-shaped concavities and silica precipitations. (d) Conchoidal fractures and breakage block features. (e) Subrounded grain with crescent steps. Pumiceous glass-shard with stretched vesicles. (f) Irregular grain with a breakage block feature. (g) Shattered glass-shard. (h) Bubble-wall glass-shard.
177x274mm (300 x 300 DPI)

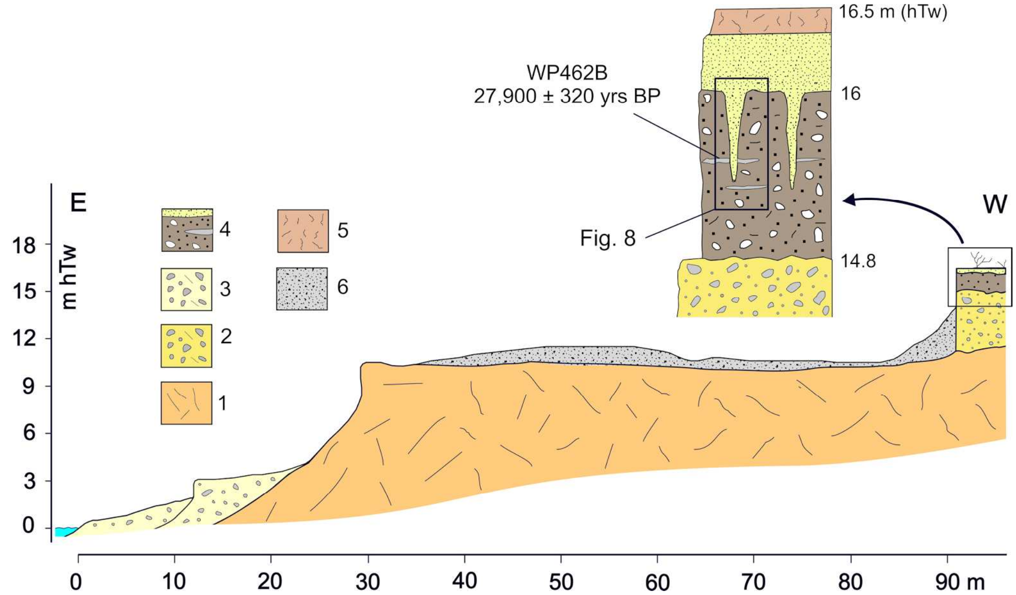


The Cantera Delgado section (WP461) (not to scale). 1: bedrock; 2: Pleistocene marine deposits; 3: Holocene marine deposits; 4: Holocene continental deposits; 5: soil; 6: quarry waste deposit. See the text for a detailed litostratigraphic description. The radiocarbon age of the pedogenetic carbonate crust is indicated. An enlargement of the sand wedge is shown in Fig. 9. Elevations are above the high tide water (hTw).
188x110mm (300 x 300 DPI)

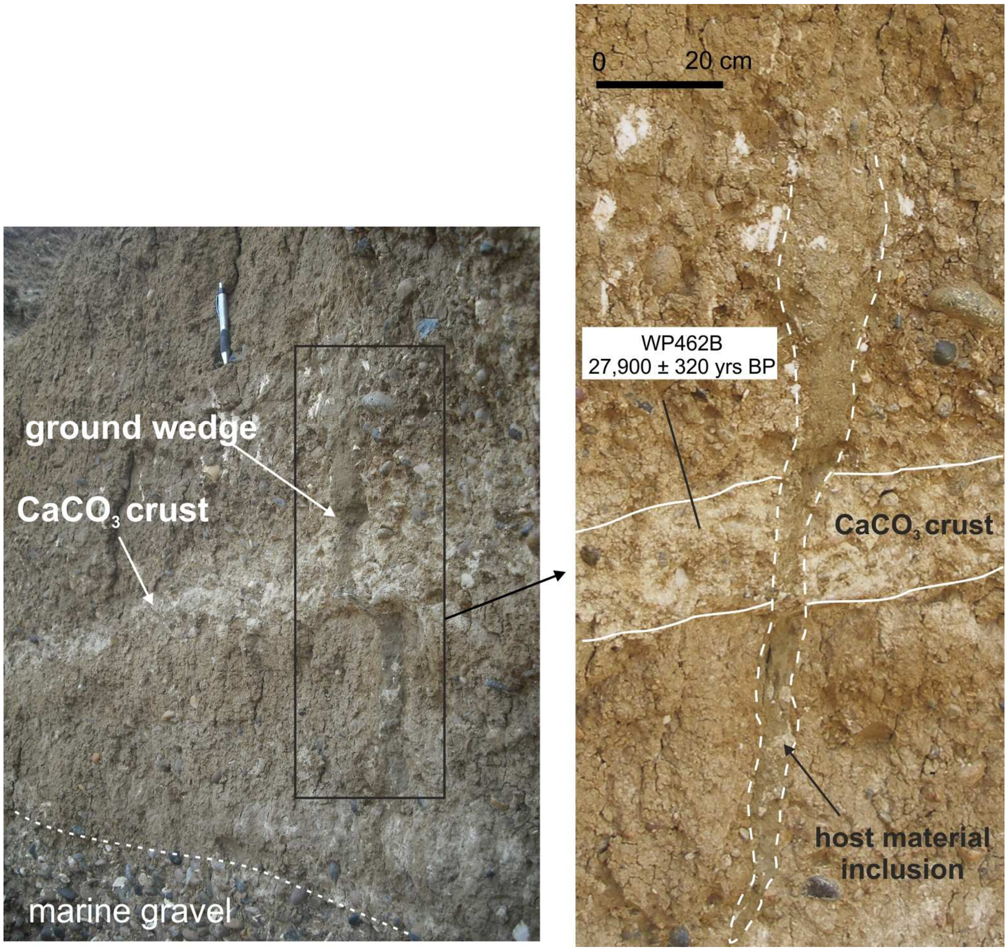


Detail of sand wedge from Fig. 8. Host material (pedogenetic crust) has moved downward as the wedge has developed. The crust yielded an OSL age of 27,900 ± 320 yrs BP.
171x161mm (300 x 300 DPI)

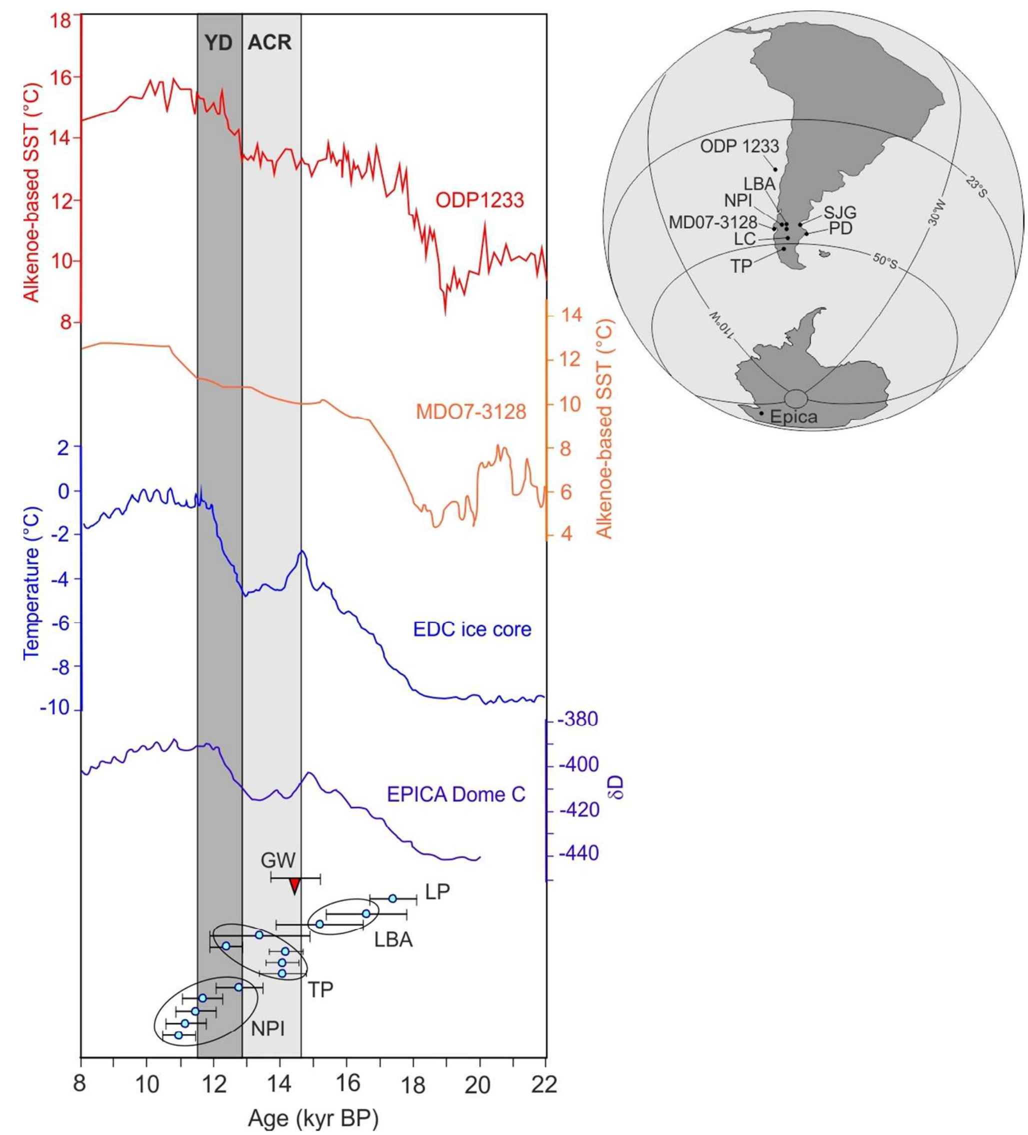


Sand wedge age (red triangle, SW) (this work) in the context of palaeoclimate information for Patagonia. Alkenone Sea Surface Temperature records are from the South Pacific cores ODP 1233 and MD07-3128. Antarctic surface temperature changes (EDC) (deviation from mean of the last millenium; Jouzel et al., 2007) plotted on the Lemieux-Dundon time-scale (Lemieux-Dundon et al., 2010). Changes of the isotopic fractionation of hydrogen in water (ice) measured at the ice core EPICA Dome C (Antarctic) (Stenni et al., 2004). Surface exposure ages of glaciers advances (blue points with uncertainty bar). LP: Lago Pueyrredon (Hein et al. 2010); LBA: Lago Buenos Aires (Hein et al. 2010); TP: Torres del Paine (Moreno et al., 2009; Fogwill and Kubick, 2005; García et al., 2012); NPI: North Patagonian Icefield (West to the Lago Buenos Aires) (Glasser at al., 2012). Ages were calculated with the Dunai time-dependent scaling scheme, adopting the isotopic production rate tested for South America (Putnam et al., 2010). YD = Younger Dryas, ACR = Antarctic Cold Reversal. In the map: SJG = St Jorge Gulf, PD = Puerto Deseado, LC = Lago Cardiel.
113x127mm (300 x 300 DPI)